M. Aizpurua, E. Garayalde, I. Lopetegi, J. Yeregui, X. Dorronsoro and U. Iraola, "Modular BESS Architecture for Enhanced Performance and Extended Lifetime," *2024 Energy Conversion Congress & Expo Europe (ECCE Europe)*, Darmstadt, Germany, 2024, pp. 1-7.

DOI: https://doi.org/10.1109/ECCEEurope62508.2024.10751995

Modular BESS Architecture for Enhanced Performance and Extended Lifetime

Manex Aizpurua
Electronics and Computing Department
Mondragon Unibertsitatea
Hernani, Spain
maizpurua@mondragon.edu

Erik Garayalde
Electronics and Computing Department
Mondragon Unibertsitatea
Hernani, Spain
egarayalde@mondragon.edu

Iker Lopetegi
Electronics and Computing Department
Mondragon Unibertsitatea
Hernani, Spain
ilopetegui@mondragon.edu

Josu Yeregui
Electronics and Computing Department
Mondragon Unibertsitatea
Hernani, Spain
jyeregui@mondragon.edu

Xabier Dorronsoro
Electronics and Computing Department
Mondragon Unibertsitatea
Hernani, Spain
xdorronsoro@mondragon.edu

Unai Iraola
Electronics and Computing Department
Mondragon Unibertsitatea
Hernani, Spain
uiraola@mondragon.edu

***Abstract*—This paper evaluates and compares the performances of non-modular and modular battery systems. The modular architecture consists of several battery modules that are individually controlled by means of their corresponding power converter. For the analysis, a realistic case study was considered, which involved a residential complex with electric vehicle chargers. Simulations were performed integrating a battery ageing prediction model. In this way, the available energy and capacity loss of the proposed system architectures were quantified under module-to-module capacity discrepancies. The capacity loss to available energy ratio was used as key performance indicator. The results demonstrate energy availability and lifetime reduction issues related to the weakest cell problem in the conventional non-modular battery. In general, the modular architecture minimises inhomogeneity effects and exhibits improved performance. Therefore, the higher cost linked to the extra power converters is expected to be compensated in large-scale applications, where the cost of the battery outweighs that of the power conversion systems.**

***Index Terms*—Modular BESS, Available energy, Ageing prediction, Battery performance.**

I. Introduction

Traditionally, battery systems are built by interconnecting cells in parallel/series until capacity and voltage requirements are fulfilled. Then, a power converter enables energy flow between the battery and the application. A Battery-Pack (BP) can consist of hundreds to thousands of cells, among which inconsistencies appear (capacity, internal resistance, etc.). These differences increase during operation time and accelerate battery ageing. Thus, Battery Management Systems (BMSs) are integrating control methodologies that reduce these inconsistencies between cells, while they supervise and protect them. Typically, passive balancing is implemented for this purpose due to its cost-effectiveness. Nevertheless, accessible energy and lifetime of the BP gets limited by the weakest cell in a serialised branch. On the other hand, active balancing circuits, rather than simply dissipating the excess energy of the strongest cells, allow it to be reallocated into weaker cells. However, this requires additional circuitry, which increases complexity and cost of the Battery Energy Storage System (BESS).

In this regard, BESSs can benefit significantly from modular designs. The outputs of several Battery Power Modules (BPMs) are interconnected here, each consisting of a substring of cells and the corresponding power converter. Modularising the Power Conversion System (PCS) enables individual control of modules. Among the different power distribution control strategies found in literature, most of them aim to equalise the State-of-Charge (SoC) of all battery modules [1]–[3] to maximise the stored energy usage. More advanced control strategies can also be applied for battery lifetime extension [4], [5], which can be combined with active thermal distribution algorithms [6].

From the perspective of functionality and versatility, modular BESSs offer additional benefits. For instance, modularity allows for easy customisation and scalability of a design for different voltage, power, and energy levels. By simply adding or subtracting BPMs when required, the size of a BESS can be optimised for different applications, thus avoiding oversizing issues. Moreover, modular BESSs have the ability to remain operational in the event of a failure, where only the defective BPM should be replaced. Lastly, modularity makes it possible to construct heterogeneous BESSs, which is attractive for applications involving second-life batteries [7].

The design and sizing processes of a modular BESS entail some important challenges. Due to the high number of power converters required, the initial cost and complexity of the system may increase. Thereby, a trade-off should be achieved to build a cost-effective solution. In [8], the authors evaluate a BESS across various levels of modularisation, examining its efficiency, cost, volume, and weight. They demonstrate that all three aspects can be optimised by selecting an adequate number of modules. Other studies have demonstrated that as modularisation levels increase, available energy of the BESS

also rises [9], [10]. However, to the best of the authors' knowledge, the impact of modularisation in battery ageing has not been analysed in the literature. In pursuit of that, this paper's primary contributions are as follows:

- Based on a realistic case study, energy availability and battery ageing of equivalent non-modular and modular BESSs are quantified under module-to-module capacity discrepancies. A degradation model is implemented in simulations to predict capacity loss due to battery cycling.
- The overall performances of non-modular and modular BESS architectures are compared using the ratio of capacity loss to discharged energy as Key Performance Indicator (KPI).

The paper is organised as follows. In Section II, the case study is introduced. Section III focuses on describing the methodology followed for the evaluation of BESS performance, and the simulation model is described. The results are illustrated and discussed in Section IV. Finally, the main conclusions of the study are presented in Section V.

II. Case Study Description

In this study, a residential community application is analysed. Four homes, a shared photovoltaic (PV) installation, a BESS, and a small Electric Vehicle (EV) charging station make up the neighbourhood. In this scenario, the battery stores surplus power from the PV system when generation exceeds consumption, and then releases it when required. The rest of the consumption is provided by the grid. An overview of the case study is presented in Figure 1.

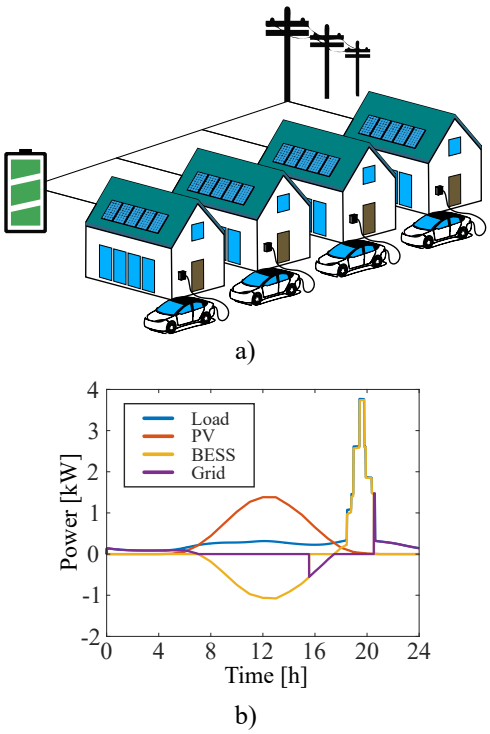

Fig. 1. Overview of the case study: a) graphical representation, b) power profiles.

The German standard load profile (SLP) H0 was used to represent the daily electricity consumption of the household [11]. Considering the whole year, the average daily profile was obtained, which was scaled to an annual consumption of 5,000 kWh/a per home.

The power generation profile for the PV system, sized to a peak power of 40 kW, was obtained by using the German Aerospace Center's (DLR) software Greenius 4.1.1 [12]. The meteorological input data corresponds to Berlin, Germany.

For the EV charging station, the traffic profile generation tool presented in [13] was used, which emulates non-deterministic traffic cases based on data from similar applications. This tool also makes it possible to simulate situations in which there is no data availability but there are set schedules, like in private companies or residential communities such the one this paper analyses. The input parameters for the generation of the traffic profile were set as follows: arrival time at 19:00, departure time at 07:30, and a total number of 4 vehicles, each with an average daily distance travelled of 40 km. Lastly, taking into account that the EV charging station comprises four chargers, each rated at 11.5 kW, the power profile was generated accordingly.

Finally, the BESS is designed with a nominal energy capacity of 60.5 kWh. It is divided into six battery modules, each with a nominal voltage and capacity of 48 V and 210 Ah, respectively. In this paper, two distinct PCS architectures, each rated for a maximum power of 39 kW for both charging and discharging, will be examined (Figure 2). On the one hand, in the conventional BESS architecture, battery modules are connected in series before they are coupled to a fixed 700 V DC bus by means of a single step-up DC-DC converter. The modular BESS, on the other hand, has six DC-DC power converters. Each of them features nominal input/output voltages of 48–350 V and a maximum power rating of 6.5 kW. A 3P-2S arrangement is used to connect two branches made up of three parallel connected BPMs in series.

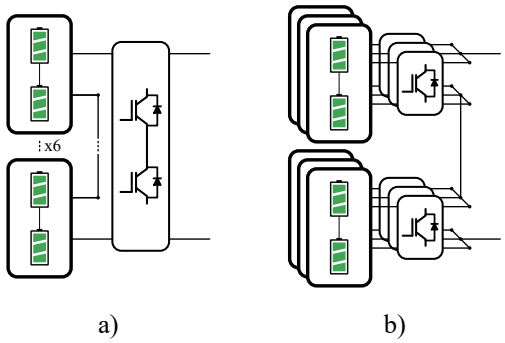

Fig. 2. BESS architectures considered for analysis: a) non-modular BESS, b) modular BESS.

III. Methodology

This section describes the method used to quantify and compare the battery ageing and accessible energy of the conventional BESS architecture against that of a modular variant,

under module-to-module inconsistencies. Their performance was simulated in Matlab/Simulink environment, and two different control strategies were considered for the modular BESS variant.

A. Performance Indicators

Two main battery performance indicators are analysed in this article:

- Discharged energy (E_{dch}): it refers to the energy that has been transferred from the BESS to the load, and it is measured in Wh.
- Capacity loss (Q_{loss}): it indicates the reduction in the ability to store and deliver charge by a battery due to ageing. It is measured in Ah. Generally speaking, the BESS's overall lifespan is limited by the single cell or module with the lowest capacity or health, particularly in those with a conventional non-modular architecture. Thus, the capacity loss of the weakest module ($Q_{\mathrm{loss,wm}}$) can have a greater effect than the capacity loss of the entire BESS as a whole ($Q_{\mathrm{loss,tot}}$).

However, it is unfair to compare capacity loss of batteries whose discharged energy was different. Therefore, to facilitate the overall performance comparison, we introduce the variable α as KPI, representing the ratio of $Q_{\mathrm{loss,tot}}$ to E_{dch} (mAh/kWh) as follows,

$$\alpha = \frac{Q_{\mathrm{loss,tot}}}{E_{\mathrm{dch}}} \ . \tag{1}$$

B. Inhomogeneities Between Modules

Battery pack performance is far inferior to cell performance due to the inevitable differences between cells. There are various factors that cause discrepancies between cells even at Beginning Of Life (BOL), such as material inconsistencies and manufacturing process issues [14]. Many authors in the literature have measured capacities and impedances of "equal" lithium-ion cells, which in most of the cases are fit to a Gaussian distribution [15]–[17] with standard deviations in capacity of up to 1.3 % at BOL.

Furthermore, at the battery pack level, inhomogeneous degradation occurs caused by differences in the operating conditions of individual cells or modules. Temperature gradients inside the battery pack [18] or uneven contacts between parallelised cells result in an inhomogeneous current flow [19], causing discrepancies between the battery units to increase during operation time.

To examine the impact of these variations on BESS ageing and accessible energy, capacity discrepancies between the battery modules were sampled considering a normal distribution as follows,

$$C \sim \mathcal{N}(210,\, \sigma^2) \ , \tag{2}$$

where σ is the standard deviation. For the analysis, the relative coefficient of variation, denoted as $k = \sigma/210$, was employed, and different values were defined: 0.5 %, 1%, 2 %, and 3%. In order to obtain convergence in the results, the process of sampling capacity discrepancies was repeated 100 times per each k value, resulting in a total number of 400 different capacity distributions. Finally, for each of the distributions, three simulations were performed: one for the conventional non-modular BESS architecture, and two for the modular variant, each with a different control strategy.

C. Battery Management and Control

Apart from supervising and protecting battery cells within a BESS, one of the primary roles of the BMS is to minimise cell-to-cell inconsistencies to maximise battery lifetime. The different battery management strategies considered in this work for the two different BESS architectures are explained below. To ensure a fair comparative analysis, a general constraint was fixed for all of the strategies: the BESS must operate within the average SoC range of 10-90 %.

1) Conventional BESS - Passive SoC balancing: Cell balancing between serialised cells can be achieved through passive or active methods [20]. Overall, although active balancing circuits offer better performance in terms of efficiency and energy accessibility, they provide only small benefits over the low-cost and straightforward hardware design of passive balancing systems. Therefore, passive balancing is still used in many commercial systems, which is why it was chosen for the analysis.

Passive balancing is typically activated at the conclusion of the charging process, since the extra heat generated when dissipating the excess energy of the strongest cells could accelerate the degradation of the battery pack. Thus, in this work, it is performed when the weakest module reaches the 90 % limit. Passive balancing is activated in modules whose SoC differs by more than 0.5% compared to the module with the lowest SoC, and remains active until all modules reach the same SoC level as the least charged module. For a typical balancing current of C/20, and based on the nominal battery module parameters, the balancing resistor was set to 4.6 ohms per module.

2) Modular BESS: Within a BESS, modularity allows for the implementation of power distribution control algorithms among battery modules. In this sense, the interconnection mode of the BPMs has a great impact. Parallel connected BPMs share the same output voltage, and as long as power limitations are not exceeded, current can be distributed as desired amongst BPMs. Instead, in the case of the series architecture, cascaded BPMs share the same load current. Voltage sharing is only achieved when the power is equally distributed among the BPMs. If not, each BPM operates at a different output voltage, therefore the power distribution control must additionally take the maximum output voltage limits of individual BPMs into account.

This is the reason why, for the 3P-2S combined modular BESS structure of the presented case study, the power distribution control strategies that are later explained are divided into two steps. First, power is distributed between the two serialised branches, and subsequently allocated among the parallel-connected BPMs within each branch. For the analysis, BPM power is limited to 6.5 kW both for charging and

discharging, and a maximum BPM output voltage variation of +15 % with regard to the nominal 350 V is considered.

Two different power distribution control strategies are analysed in this paper, whose main objectives are the following:

i) Active SoC balancing: as commonly done in literature [1]–[3], this control strategy intends to continuously equalise the SoC of all the BPMs throughout the charging or discharging periods of the BESS. BESS power is set to zero when any of the modules exceeds the 10-90 % SoC range.

ii) Life extension control: based on the work presented in [4], this control aims to equalise the State of Health (SoH) of all the battery modules. To this end, the operable SoC range of each module is modified depending on their SoH or accessible capacity. Higher-capacity modules operate at a wider SoC range. BESS power is set to zero when the average BESS SoC exceeds the 10-90 % SoC range.

Further details regarding the implementation of these two controls can be found in the Appendix.

D. BESS Simulation Model

Simulations were performed in the MATLAB/Simulink environment, operating with a sample time of 1 second.

1) PCS Model: Although DC-DC converters have high-frequency dynamics, for the analysis only their static behaviour was contemplated. Moreover, power conversion was considered lossless. Therefore, the battery current was determined by dividing the instantaneous power reference set by the control with the instantaneous battery voltage.

In the non-modular BESS, battery modules were initially connected in series, resulting in a battery voltage equal to the sum of individual module voltages and a unique power reference for the power converter. On the contrary, in the case of the modular BESS configuration, each BPM possessed its own power reference, leading to varying currents.

2) Battery Model: To represent the dynamics of the BESS, battery voltage and SOC, the generic battery model integrated in the Simscape library was used [21]. Each of the six modules that constitute the BESS was simulated by an equivalent unique cell model of 210 Ah nominal capacity and 48 V module voltage. However, as discussed before in Section III-B, the inserted module capacity was adjusted around the nominal value to simulate and analyse the impact of capacity variations on BESS performance.

To predict BESS degradation, the semi-empirical model presented in [22] was applied. Capacity loss was characterised by two main phenomena: calendar ageing and cycling ageing. In this work, since short battery operation times were simulated (up to 1 week), calendar ageing was neglected. Regarding cycling ageing prediction, this model operates on the basis of charge throughput rather than the conventional approaches of adding Depth of Discharge (DoD) and cycle number dependence as follows:

$$\begin{aligned} Q_{\text{loss}} &= \int k_{\text{HiqhT}}(T) \cdot \left(2\varphi^{0.5}\right)^{-1} d\varphi_{\text{Tot}} \\ &+ \int k_{\text{LowT}}\left(T, I_{\text{Ch}}\right) \cdot \left(2\varphi^{0.5}\right)^{-1} d\varphi_{\text{Ch}} \\ &+ \int k_{\text{LowT,HighSoC}}\left(T, I_{\text{Ch}}, SoC\right) d\varphi_{\text{Ch}} \ . \end{aligned} \tag{3}$$

The stress factors k_{HighT} , k_{LowT} and $k_{\text{LowT,HighSoC}}$ indicate the dependence of the capacity loss resulting from distinct operational conditions. Then, φ denotes the battery charge throughput, with φ_{Ch} representing the charge only for the battery charging scenario and φ_{Tot} representing the total charge taking into account both the charge and the discharge.

Stress factor values were acquired from [22], which correspond to the 3 Ah Lithium Iron Phosphate US26650FTC1 battery cell. Thus, the module current input for the degradation model was adapted dividing it by a factor of 70, assuming that 70 cells need to be connected in parallel to reach the nominal 210 Ah capacity. Finally, it was assumed that all modules operate at the same temperature of 25 °C.

IV. Results

An entire week was simulated to obtain the results. Figure 3 shows the statistical distributions of 400 simulations for each of the BESS variants. The circular marker indicates the median value, while the grey vertical bar represents the interquartile range.

A. Discharged Energy

The weakest cell problem is apparent for the traditional non-modular BESS architecture. Energy accessibility decreases as the standard deviation increases. Instead, the modular BESS architecture, regardless of the battery management strategy, is capable of accessing all the available energy at the module level. The total accessible energy increased by up to 1.3 % and 11.6 % for standard deviations of 0.5 % and 3 %, respectively. Moreover, compared to the non-modular BESS, the deviation of the results decreases.

B. Capacity Loss

The total loss of BESS capacity is greater for modular BESS variants. In the case of the non-modular BESS, since it is not accessed to the entire energy of the BESS, the strongest battery modules operate with lower depth of discharge. Thus, capacity loss in those strong modules is smaller than in the cases of the modular solutions. However, focusing on the weakest module, it happens the other way around. The non-modular BESS exhibits the largest $Q_{\text{loss,wm}}$, which leads to a shortened overall lifespan.

As for the modular BESS management strategies, the life extension control is capable of reducing capacity loss in the weakest module by up to 2.3 % and 13.7 % for standard deviations of 0.5 % and 3 %, respectively. However, doing so causes the stronger modules to age more quickly. For that reason, there is no visual difference in total BESS capacity

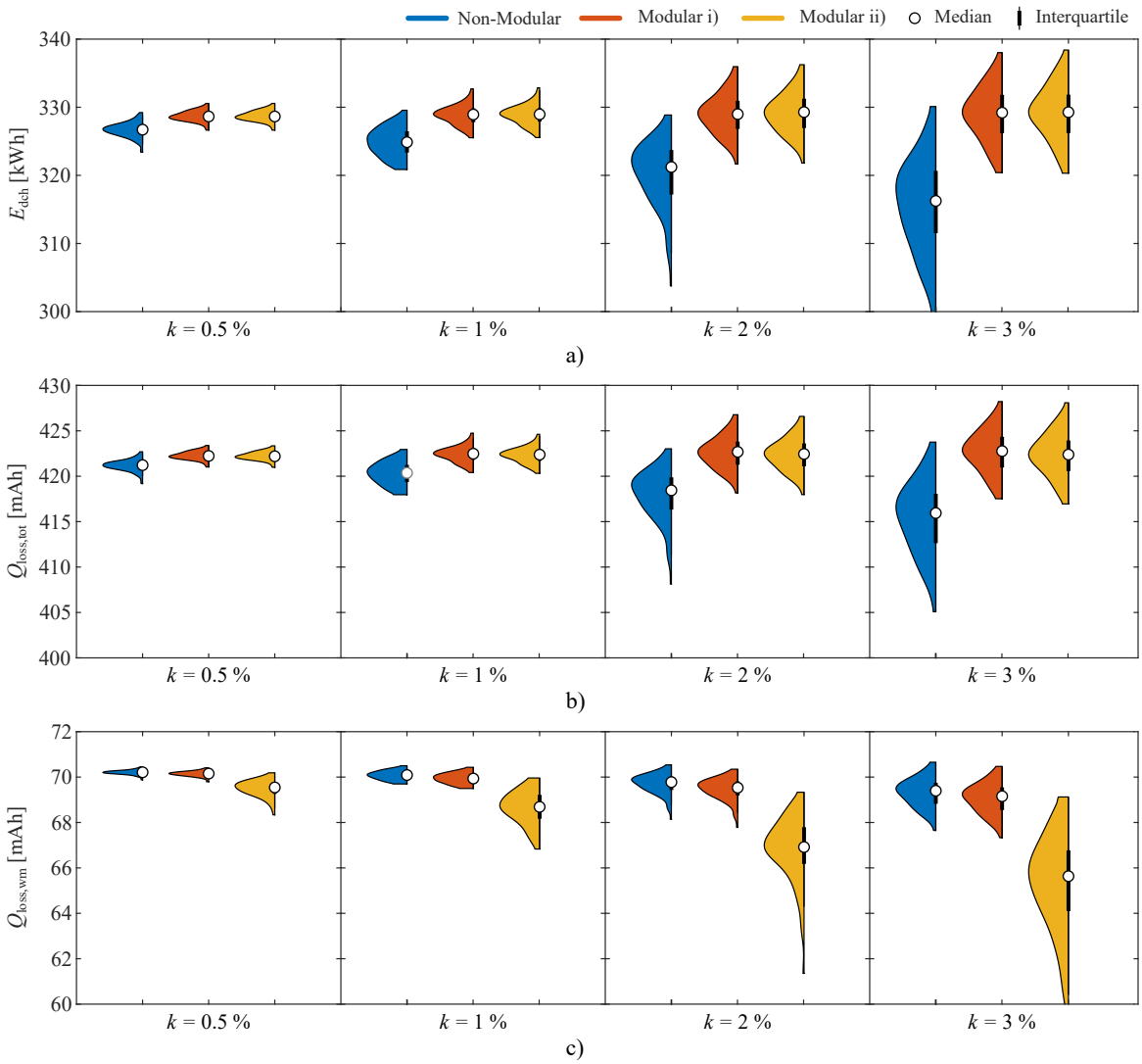

Fig. 3. Statistical distributions of the results from 400 simulations per BESS variant. Simulations were initialised by sampling 100 different capacity distributions for each k value. a) Discharged energy, b) Total capacity loss of the BESS, c) Capacity loss of the weakest module.

loss between the aforementioned control strategy and the SoC balancing method.

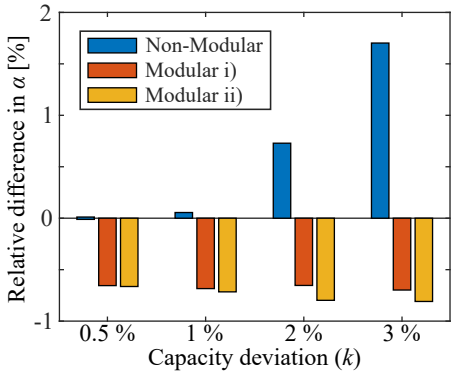

Fig. 4. Overall performance comparison of the analysed BESS variants. The relative differences of α are plotted taking the non-modular BESS with $k = 0.5$ % as the baseline.

C. Overall Performance

The overall performance comparison is shown in Figure 4. Median values are considered, since they closely correspond to the most populated point in the distribution.

The modular architecture is shown to outperform the conventional non-modular BESS in all circumstances, with the understanding that a lower α indicates a higher performance. KPI α improved by 0.7 % and 2.5 % for standard deviations of 0.5 % and 3 %, respectively. Moreover, performance keeps relatively constant despite increased capacity variations, while in the case of the non-modular BESS it decreases exponentially.

With this in mind, it is expected for the modular BESS architecture to keep its performance level relatively constant over the entire BESS lifetime. Instead, performance will decrease considerably for the non-modular BESS, assuming that inhomogeneities between modules increase during their

operating life.

D. Discussion

While modular BESSs provide better performance than non-modular counterparts in aspects of energy accessibility and battery degradation, the modular approach generally leads to higher costs owing to the increased number of power converters. Therefore, analysing the cost breakdown of present BESSs is crucial to identify potential applications.

This paper focuses on rather small BESS ratings corresponding to a residential application. Cost details of current residential, commercial, and utility-scale BESSs are depicted in Figure 5. Data is collected from [23] (last updated in 2023), which uses the NREL's bottom-up cost model [24]. For easier understanding and clarity, only costs related to the lithium-ion battery and power conversion components are detailed, which are directly influenced by the adopted BESS configuration. It is observed that their costs in the case of residential BESSs are comparable. However, in the case of larger BESSs, the cost of the battery significantly outweighs that of the power converters, exceeding it by more than a factor of ten. Thus, it is concluded that adopting a modular BESS configuration is more advantageous for energy applications with larger battery systems, as the increase in power conversion system costs has a minimal effect on the overall BESS cost, which is expected to be offset by the benefits in performance.

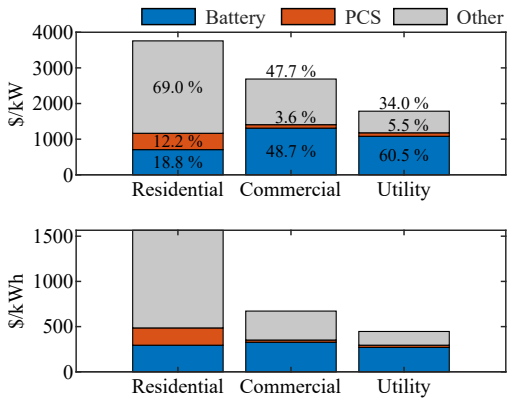

Fig. 5. Cost details of 5 kW/12 kWh residential, 300 kW/1.2 MWh commercial, and 60 MW/240 MWh utility-scale BESSs. Data from [23].

Although this work concentrates on a DC-coupled BESS, in many of today's applications batteries are coupled to an AC link. In such scenarios, PCSs are classified in two-stage and single-stage architectures. Two-stage PCSs consist of an initial DC-DC conversion stage that is followed by an inverter. The DC-DC stage offers great flexibility and control over the battery modules constituting the modular BESS, specially when connected in parallel. However, the extra conversion step may reduce the compactness and increase costs. Instead, in single-stage PCSs batteries are directly connected to the AC link through an inverter. In this context, although they are beyond the scope of this work, modular multilevel converter architectures are seen as promising future solutions, with research needing to focus on developing power sharing algorithms to enhance the control of individual battery modules [25].

Finally, in addition to the previously quantified performance gain, the modular BESS approach provides further qualitative benefits that should be noted again. The capability to control each battery module independently facilitates the integration of battery modules with significant differences into the same BESS, thus creating a heterogeneous system. This can be of particular interest for the second life battery market. Other benefits are related to the sizing process of the BESS. Modular BESSs can be scalable and fault-tolerant, meaning that an existing system can be expanded by adding new modules as needed, and faulty modules can be replaced without further impact in case of failure.

V. Conclusions

This article examines the overall performance of a BESS with capacity disparities between modules, taking into account different architectures: non-modular versus modular. Modular BESSs consist of multiple interconnected power converters, each controlling an independent battery module, while in the conventional non-modular architecture, a single power converter is employed for the entire higher voltage battery pack.

A practical case study that includes an EV charging station in a residential complex was considered. Energy accessibility and battery ageing were quantified via simulations, and the ratio between the two terms was used as KPI to compare the overall BESS performance.

The results evidence energy accessibility issues related to the weakest cell problem in conventional non-modular BESSs. Higher capacity discrepancies between modules led to reduced discharged energy. Instead, the BESS of modular structure is capable of accessing the total energy in all cases. Due to this, the total BESS capacity loss is higher in the case of the latter. Even so, lifetime of the non-modular BESS is generally defined by the weakest cell. The highest weakest cell capacity loss is given by the non-modular BESS. Thus, an extended lifetime is expected by adopting a modular BESS.

Overall, the BESS of the modular architecture exhibits enhanced performance. The KPI remains essentially constant regardless of the module-to-module capacity discrepancies for the modular BESS, while it decreases exponentially for the non-modular BESS. Moreover, further improvement is anticipated through the implementation of cutting-edge power distribution control strategies in modular batteries, currently under research. Thus, the increased cost associated with the additional power converters is expected to be offset by the benefits of the modular approach, especially in large-scale batteries, where the battery's cost is substantially higher than that of the PCS.

Acknowledgment

This research did not receive any specific grant from funding agencies in the public, commercial, or not-for-profit sectors.

REFERENCES

[1] Y. Li and Y. Han, "A module-integrated distributed battery energy storage and management system," *IEEE Transactions on Power Electronics*, vol. 31, no. 12, pp. 8260–8270, 2016.

[2] M. Kamel, V. Sankaranarayanan, R. Zane, and D. Maksimović, "State-of-charge balancing with parallel and series output connected battery power modules," *IEEE Transactions on Power Electronics*, vol. 37, no. 6, pp. 6669–6677, 2022.

[3] M. Crespo, I. Peláez, P. García, R. Georgious, C. Blanco, and I. Cantero, "Series/parallel li-ion battery modules active equalisation considering load and no-load operation," *IEEE Transactions on Industry Applications*, vol. 59, no. 3, pp. 3493–3503, 2023.

[4] M. M. U. Rehman, *Modular, Scalable Battery Systems with Integrated Cell Balancing and DC Bus Power Processing*, 2018.

[5] M. Bauer, M. Muehlbauer, O. Bohlen, M. A. Danzer, and J. Lygeros, "Power flow in heterogeneous battery systems," *Journal of Energy Storage*, vol. 25, p. 100816, 2019.

[6] Y. Li and Y. Han, "A new perspective on battery cell balancing: Thermal balancing and relative temperature control," in *2016 IEEE Energy Conversion Congress and Exposition (ECCE)*, 2016, pp. 1–5.

[7] N. Mukherjee and D. Strickland, "Control of second-life hybrid battery energy storage system based on modular boost-multilevel buck converter," *IEEE Transactions on Industrial Electronics*, vol. 62, no. 2, pp. 1034–1046, 2015.

[8] M. Bauer, J. Wiesmeier, and J. Lygeros, "A comparison of system architectures for high-voltage electric vehicle batteries in stationary applications," *Journal of Energy Storage*, vol. 19, pp. 15–27, 2018.

[9] X. Dorronsoro, I. Lopetegi, E. Garayalde, U. Iraola, and J. Yeregui, "Modular battery energy storage systems for available energy increase," in *2022 IEEE Vehicle Power and Propulsion Conference (VPPC)*, 2022, pp. 1–7.

[10] D. F. Frost, *Battery management systems with active loading and decentralised control*, 2017.

[11] Bdew, "Federal association of the german energy and water industries, standard load profile h0," (accessed 13 February 2024). [Online]. Available: https://www.bdew.de/energie/standardlastprofile-strom/

[12] German Aerospace Center (DLR), "Greenius - the green energy system analysis tool," (accessed 13 February 2024). [Online]. Available: https://www.dlr.de/sf/en/desktopdefault.aspx/tabid-11688/20442_read-44865/

[13] J. Yeregui, J. Urkizu, and I. Aizpuru, "Data-based traffic profile generation tool for electric vehicle charging stations," in *2023 IEEE Vehicle Power and Propulsion Conference (VPPC)*, 2023, pp. 1–6.

[14] D. Beck, P. Dechent, M. Junker, D. U. Sauer, and M. Dubarry, "Inhomogeneities and cell-to-cell variations in lithium-ion batteries, a review," *Energies*, vol. 14, no. 11, 2021.

[15] S. Lehner, T. Baumhöfer, and D. U. Sauer, "Disparity in initial and lifetime parameters of lithium-ion cells," *IET Electrical Systems in Transportation*, vol. 6, no. 1, pp. 34–40, 2016.

[16] S. Paul, C. Diegelmann, H. Kabza, and W. Tillmetz, "Analysis of ageing inhomogeneities in lithium-ion battery systems," *Journal of Power Sources*, vol. 239, pp. 642–650, 2013.

[17] K. Rumpf, M. Naumann, and A. Jossen, "Experimental investigation of parametric cell-to-cell variation and correlation based on 1100 commercial lithium-ion cells," *Journal of Energy Storage*, vol. 14, pp. 224–243, 2017.

[18] K.-C. Chiu, C.-H. Lin, S.-F. Yeh, Y.-H. Lin, C.-S. Huang, and K.-C. Chen, "Cycle life analysis of series connected lithium-ion batteries with temperature difference," *Journal of Power Sources*, vol. 263, pp. 75–84, 2014.

[19] L. Wang, Y. Cheng, and X. Zhao, "Influence of connecting plate resistance upon lifepo4 battery performance," *Applied Energy*, vol. 147, pp. 353–360, 2015.

[20] S. W. Moore and P. J. Schneider, "A review of cell equalization methods for lithium ion and lithium polymer battery systems," 2001.

[21] O. Tremblay and L.-A. Dessaint, "Experimental validation of a battery dynamic model for ev applications," *World Electric Vehicle Journal*, vol. 3, no. 2, pp. 289–298, 2009.

[22] M. Schimpe, M. E. von Kuepach, M. Naumann, H. C. Hesse, K. Smith, and A. Jossen, "Comprehensive modeling of temperature-dependent degradation mechanisms in lithium iron phosphate batteries," *Journal of The Electrochemical Society*, vol. 165, no. 2, p. A181, jan 2018.

[23] NREL, "Anual technology baseline," (accessed 24 May 2024). [Online]. Available: https://atb.nrel.gov/electricity/2023/technologies

[24] V. Ramasamy, J. Zuboy, E. O'Shaughnessy, D. Feldman, J. Desai, M. Woodhouse, P. Basore, and R. Margolis, "U.S. solar photovoltaic system and energy storage cost benchmarks, with minimum sustainable price analysis: Q1 2022," 2022.

[25] F. Díaz-González, D. Heredero-Peris, M. Pagès-Giménez, E. Prieto-Araujo, and A. Sumper, "A comparison of power conversion systems for modular battery-based energy storage systems," *IEEE Access*, vol. 8, pp. 29 557–29 574, 2020.

APPENDIX

As stated in Section III-C, two alternative control strategies were considered to distribute the total BESS power P between the modules that make up the modular BESS variant.

i) Active SoC balancing: power distribution between N serialised branches is determined by (4), and (5) is applied for the parallel connected M modules inside a branch. The values for the constants k_1 and k_2, were 3 and 650 accordingly.

$$P_n = P/N \cdot (1 \pm k_1 \cdot (SoC_n - \overline{SoC})) \quad n \in \{1, 2...N\} \quad (4)$$

$$P_m = P/M \pm k_1 \cdot (SoC_m - \overline{SoC})) \quad m \in \{1, 2...M\} \quad (5)$$

ii) Life extension control: power is distributed following the same expressions between serialised branches and parallel connected modules. First, SoC ranges of the I modules are defined as follows,

$$SoC_{i,\max} = 90\% + k3 \cdot (C_i - \overline{C}) \quad i \in \{1, 2...I\}\,, \quad (6)$$

$$SoC_{i,\min} = 10\% - k3 \cdot (C_i - \overline{C})\,, \quad (7)$$

where, k_3 equals 125, and C indicates the maximum capacity of a battery module.

Then, in each of the iterations, based on the difference between the instantaneous SoC of a module (SoC_i) and its upper/lower limit, the remaining capacity to charge/discharge $C_{i,\mathrm{rem}}$ is estimated,

$$C_{i,\mathrm{rem}} = \begin{cases} (SoC_{i,\max} - SoC_i) \cdot C_i & , P < 0 \\ (SoC_i - SoC_{i,\min}) \cdot C_i & , P > 0 \end{cases}\,. \quad (8)$$

Finally, power distribution is defined by,

$$P_i = P \cdot \frac{C_{i,\mathrm{rem}}}{\sum_{i=1}^{I} C_{i,\mathrm{rem}}}\,. \quad (9)$$